On the role of modelling uncertainty in optimal control and performance assessment of wave energy conversion systems

On the role of modelling uncertainty in optimal control and performance assessment of wave energy conversion systems

Conference Paper · June 2024

CITATIONS
0

READS
15

2 authors:

Nicolás Faedo
Politecnico di Torino
116 PUBLICATIONS **1,431** CITATIONS
SEE PROFILE

Maria Luisa Celesti
Politecnico di Torino
5 PUBLICATIONS **4** CITATIONS
SEE PROFILE

Proceedings of the Thirty-fourth (2024) International Ocean and Polar Engineering Conference **www.isope.org**
Rhodes, Greece, June 16–21, 2024

ISBN 978-1-880653-78-4; ISSN 1098-6189

On the role of modelling uncertainty in optimal control and performance assessment of wave energy conversion systems

Nicolás Faedo and Maria Luisa Celesti
Marine Offshore Renewable Energy Lab, Politecnico di Torino, Turin, Italy

ABSTRACT

Modelling uncertainty can play a fundamental role in optimal control design for wave energy converters (WECs), with potentially drastic results predicted within the literature, if not considered and incorporated into the synthesis procedure appropriately. Most of these hypothesised situations, nonetheless, are conducted on the basis of modelling uncertainty generated synthetically, *e.g.* by assuming numerically produced parameter/system variations, precluding a realistic assessment of the effect of uncertainty arising from actual experimental conditions. To fill this gap, within this paper, modelling and uncertainty characterisation are performed fully based on experimental data, with tests designed specifically to extract information on the response of a prototype WEC system under different operating conditions. With the computed family of models, the energy-maximising control problem is solved by leveraging so-called moment-based theory, in both nominal and robust control frameworks.

KEY WORDS: Wave energy, Robust control, Uncertainty

INTRODUCTION

While effectively representing a vast renewable resource, ocean wave energy is yet largely untapped: Technology convergence has not yet been achieved, with thousands of patents proposed in the last decades, ostensibly due to the substantial variability between operating conditions in different sites among the globe (Clément et al., 2002). In other words, mostly in line with wave conditions, certain wave energy converter (WEC) concepts might be deemed more suitable, making the transition towards standardisation a rather difficult task. A fundamental tool, which relatively quickly became popular to 'adapt' WEC systems to diverse sites and conditions, hence contributing to the pathway towards concept convergence, is the use of appropriate control technology (Ringwood et al., 2023b). In particular, the core role of control in wave energy is that of maximising the energy absorbed from the incoming wave field in a wide variety of wave conditions, while systematically guaranteeing technological limitations, hence both maximising the raw profit obtained for any given WEC concept, and minimising the need for repeated maintenance intervention. This, consequently, improves the overall cost-efficiency of the converter, minimising the associated levelised cost of energy (LCoE).

Though a recognised key stepping stone, the design and synthesis of control technology for WEC systems is known to be significantly challenging. Most of the available state-of-the-art techniques, able to both maximise energy conversion and guarantee constraint satisfaction, are model-based, *i.e.* they necessitate a dynamical description of the WEC device under analysis. Even if a mathematical model is effectively derived, given that the formulation of the control problem itself leads to branches within the field of optimal control theory, an online optimisation is virtually always required (see *e.g.* (Pasta et al., 2023)), which automatically imposes a hard limit in the computational and analytical complexity of the mathematical model used for control purposes. As a consequence, the vast majority of the literature is based on (nominal) linear WEC representations, derived under the assumption of infinitesimally small device motion, *i.e.* a constant still water level (SWL), in an effort to compute control solutions with practical relevance, that is, with real-time capabilities.

This set of assumptions, known as linear potential flow theory (Korde and Ringwood, 2016), is intrinsically limiting, creating what is nowadays referred to as the *WEC modelling paradox* (Windt et al., 2021): While, within these assumptions, modelling is performed with the hypothesis of infinitesimally small motion, the control system itself often tries to exaggerate device displacement to maximise absorbed energy, driving the WEC well beyond linearity conditions. This creates an uncertainty 'cycle' between nominal device representation and associated synthesised controller, shown to lead to drastic scenarios, with even negative overall power absorption (Bacelli et al., 2015; Faedo et al., 2022a).

In an effort to avoid this, modelling uncertainty can be quantified and parameterised accordingly, generating an associated family of WEC models, as opposed to a single (nominal) mathematical structure (Celesti et al., 2024; Farajvand et al., 2023). Such a set of systems can be used both for pure performance assessment purposes, for controllers based on a nominal model (as per the vast

majority of the state-of-the-art), and for design and synthesis of (more suitable) robust control design techniques. Though rather scarce and often limited in practical relevance, examples pertaining to the latter can be found in (Faedo et al., 2022b; Garcia-Violini and Ringwood, 2021; Zhang and Li, 2022). Nonetheless, up to date, characterisation of uncertainty for control purposes has been limited to simulation studies, *i.e.* a family of WEC models is generated based on synthetic data only, precluding a realistic assessment of the effect of modelling inaccuracies in control synthesis and corresponding performance. This would provide actual confirmation of some of the extreme scenarios found in simulation for control techniques solely based on nominal WEC representations, and provide conclusive information on the role and relevance of uncertainty, even at a preliminary design stage.

To fill this gap, this paper aims to address each fundamental stage in the overall process: Modelling and uncertainty characterisation is performed fully based on experimental data, with tests designed specifically to extract information on the response of a prototype WEC system under different operating conditions. The chosen device is a 1:20 scale prototype of the so-called Wavestar system (Hansen and Kramer, 2011), tested in the wave facilities available at Aalborg University, Denmark, as part of a larger experimental campaign (Faedo et al., 2023). With the computed family of models, the WEC energy-maximising control problem is solved by leveraging so-called moment-based theory (Faedo and Ringwood, 2023), in both nominal and robust control frameworks. Moment-based control, which has shown to be effective in solving the WEC control problem efficiently (including experimental validation for single devices and even array configurations) essentially constitutes a direct optimal control technique, able to transcribe the energy-maximising infinite-dimensional problem to a tractable finite-dimensional nonlinear program (NP). Within this paper, leveraging such a control framework, we provide the following key outcomes:

- Optimal controllers solely based on nominal WEC representations can effectively lead to drastic scenarios, with both (a) suboptimal energy absorption (often even being negative, *i.e.* the device drains energy from the grid, as opposed to generating), and (b) inability to guarantee technological limitations, potentially leading to increased device fatigue due to inconsistent constraint satisfaction, affecting scheduled maintenance and reducing the overall lifetime of the device.
- Within a suitable mathematical framework, informing the control synthesis procedure on the existence of uncertainty, and a corresponding set of suitably defined bounds, guarantees a consistent energy absorption performance, with systematic constraint satisfaction, hence recovering the role of this technology in reducing the LCoE.

The remainder of this paper is organised as follows. Section "Notation" introduces the mathematical notation and a set of convenient operators, used within the formal treatment of the problem. Section "Device and uncertainty description" describes the experimental device considered, including the corresponding set of tests performed within the wave basin facilities, and a suitable characterisation of uncertainty, leading to a family of WEC models for the considered prototype. Section "Nominal and robust control design" introduces the control framework considered, *i.e.* moment-based direct transcription, in both nominal and robust scenarios, leveraging the uncertainty sets derived in Section "Device and uncertainty description" , while Section discusses the core numerical results of this study. Section "Conclusions" encompasses the outcomes of this paper.

Notation

$\mathbb{R}^+$ denotes the set of non-negative real numbers, while $\mathbb{C}^0$ denotes the set of pure-imaginary complex numbers. The symbol 0 stands for any zero element, conformable according to the context. The symbol $\mathbb{I}_n$ denotes the identity matrix in $\mathbb{C}^{n\times n}$. The superscript $^\mathsf{T}$ denotes the transposition operator. The notation $\mathbb{N}_N \subset \mathbb{N}$ indicates the set of natural numbers up to N, *i.e.* $\mathbb{N}_N = \{1, 2, \dots, N\}$. The spectrum of a matrix $A \in \mathbb{R}^{n\times n}$, *i.e.* the set of its eigenvalues, is denoted by $\lambda(A)$. Let $\mathscr{A}$ represent a set of square matrices with well-defined dimensions. The direct sum operator over $\mathscr{A}$ is denoted as $\bigoplus_{i\in\mathbb{N}_N} A_i = \mathrm{diag}(A_1, \dots, A_N)$, where $A_i \in \mathscr{A}$ and $N = \#\mathscr{A}$. $M_1 \otimes M_2$ denotes the Kronecker product between two matrices M_1 and M_2. Given two functions f_1 and f_2 in $L^2(\mathscr{I})$, $\mathscr{I} \subseteq \mathbb{R}$, their canonical inner-product is denoted as $\langle f_1, f_2\rangle_{\mathscr{I}} = \int_{\mathscr{I}} f_1(\tau) f_2(\tau) \mathrm{d}\tau$. The Laplace transform of $f(t)$ (provided it exists), is denoted with the corresponding capital letter, *i.e.* $F(s)$. With some abuse of notation, the Fourier transform is written as the restriction of $F(s)$ on $\mathbb{C}^0$, *i.e.* $F(\jmath\omega)$, where $s = \sigma + \jmath\omega$. Standard notation is used for Hardy spaces, *i.e.* $\mathcal{H}_\infty$ is used for the set of analytic and bounded $\mathcal{L}_\infty$ functions on the open right-half complex plane, while $\mathcal{RH}_\infty$ is the real rational subspace of $\mathcal{H}_\infty$. Let $x = [x_1, \dots x_n]^\mathsf{T} \in \mathbb{C}^n$. To conclude this preliminary section, we define the following two useful operators. The operator $\mathscr{R} : \mathbb{C}^n \to \mathbb{R}^{2n}$, as

$$\mathscr{R}(x) = \begin{bmatrix} \Re(x_1) & \Im(x_1) & \dots & \Re(x_n) & \Im(x_n) \end{bmatrix}^\mathsf{T}, \tag{1}$$

where $\Re(\circ)$ and $\Im(\circ)$ stand for the real and imaginary part of $\circ \in \mathbb{C}$. Note that (1) represents the linear isomorphism $\mathbb{C}^n \simeq \mathbb{R}^{2n}$. Finally, we define the operator $\mathscr{B} : \mathbb{C}^n \to \mathbb{R}^{2n\times 2n}$ as

$$\mathscr{B}(x) = \bigoplus_{k\in\mathbb{N}_n} \begin{bmatrix} \Re(x_k) & \Im(x_k) \\ -\Im(x_k) & \Re(x_k) \end{bmatrix}. \tag{2}$$

DEVICE AND UNCERTAINTY DESCRIPTION

The device considered for this case study, presented in Figure 1, is a prototype of the so-called Wavestar WEC system, developed in-house at Aalborg University, Denmark. In the following, we provide a brief description of the prototype for completeness, with emphasis on its configuration and reference point for modelling. The interested reader is referred to (Faedo et al., 2023) for a full description of the device and working principle.

The system is composed of a semi-spherical floater, attached to a corresponding arm, fixed at the reference point (considered for modelling purposes) described within Figure 1. A linear motor/generator, sitting on the top part of the structure, acts as a power take-off (PTO) system, exerting an associated moment u at the corresponding input point. The prototype is equipped with suitable instrumentation, able to measure linear and rotational motion, as well as total force acting on the PTO axis, being able to derive a measure of the associated wave excitation torque d for control and simulation purposes, by means of tailored testing (see (Faedo et al., 2023)). The set of tests, *i.e.* waves, required for modelling, uncertainty characterisation, and performance assessment, is fully generated within the wave basin, by means of a mechanical wavemaker, available at Aalborg facilities.

Following previous theoretical and experimental control developments in the state-of-the-art literature considering this spe-

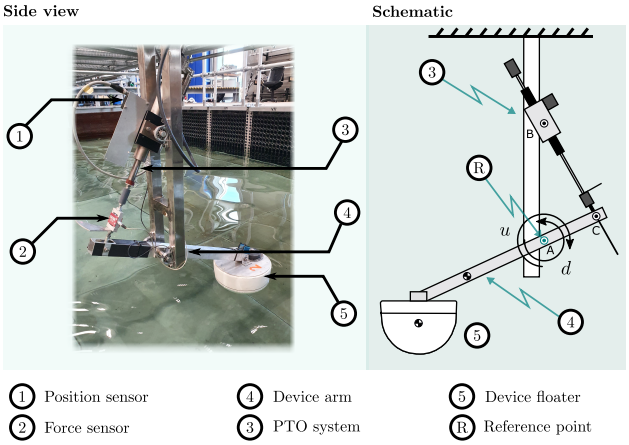

Fig. 1 Wavestar prototype considered for experimental modelling and characterisation of the corresponding uncertainty.

cific Wavestar system (see (Ringwood et al., 2023a)), within this study, the nominal dynamical model describing the WEC prototype, with respect to the reference point defined in Figure 1, is defined in terms of a linear operator $G_0 \in \mathcal{RH}_\infty$, $s \mapsto G_0(s)$, which characterises the input/output (I/O) relation

$$Y(s) = G_0(s)\,(D(s) - U(s))\,, \tag{3}$$

where $d(t) \in \mathbb{R}$ denotes the wave excitation torque acting on the device, generated by the pressure exerted on the wetted surface of the WEC as a direct action of the incoming wave field, $u(t) \in \mathbb{R}$ is the user-defined PTO (control) torque, and $y(t) \in \mathbb{R}$ denotes the device angular velocity, which is set as the main output of the system, due to its inherent relevance in the associated optimal control synthesis procedure (see Section "Nominal and robust control design").

To provide a more consistent and complete dynamical representation for the prototype WEC described in this section, and following the framework pursued in (Celesti et al., 2024), a family of (uncertain) linear time-invariant (LTI) models is considered, *i.e.* the 'true' map $G : (d-u) \mapsto y$ representing the Wavestar device is assumed to belong to a family of systems $\mathcal{G} \subset \mathcal{H}_\infty$, described by means of an unstructured uncertainty set

$$\mathcal{D} : \{\Delta \in \mathcal{H}_\infty \;\mid \|\Delta\|_\infty < 1\,\}. \tag{4}$$

Considering the definition in (4), and a corresponding additive uncertainty scheme, the family $\mathcal{G}$ can be fully defined as

$$\mathcal{G} : \{G \in \mathcal{H}_\infty \;\mid G = G_0 + W_\Delta \Delta\,\}, \tag{5}$$

where W_Δ is the weight characterising the additive uncertainty.

Following (Celesti et al., 2024), the experimental characterisation of the WEC family (5) is performed in terms of a set of Q suitable input (torque) signals $\mathscr{F} = \{f_i(t)\}_{i\in\mathbb{N}_Q}$, producing an associated set of angular velocity outputs $\mathscr{Y} = \{y_i(t)\}_{i\in\mathbb{N}_Q}$. With these two sets, a characterisation of the I/O behaviour of the actual WEC system G can be computed in terms of the so-called empirical transfer function estimate (ETFE), for each individual I/O test, *i.e.*

$$\bar{G}_i(\jmath\omega) = \frac{Y_i(\jmath\omega)}{F_i(\jmath\omega)}, \quad i \in \mathbb{N}_Q. \tag{6}$$

As a matter of fact, the associated set of ETFEs $\{\bar{G}_i\}$ encodes information of both the nominal model G_0, and the corresponding uncertainty weight W_Δ, required to define the family of systems $\mathcal{G}$ in (5). In particular, the nominal model can be computed in terms of the average ETFE $\bar{G}_0$, defined as

$$\bar{G}_0(\jmath\omega) = \frac{1}{Q}\sum_{i\in\mathbb{N}_Q} \bar{G}_i(\jmath\omega). \tag{7}$$

With the knowledge of (7), a parametric approximation can be computed leveraging standard frequency-domain system identification procedures (see (Ljung, 1999)), *i.e.*

$$G_0(s) \leftarrow \min_{G_0\in\mathcal{RH}_\infty} \left\|G_0(\jmath\omega) - \bar{G}_0(\jmath\omega)\right\|_2^2. \tag{8}$$

where, due to the physical properties of the WEC process, the identified nominal model G_0 is minimal, strictly proper, stable, and minimum-phase (see *e.g.* (Faedo et al., 2022c; Scruggs et al., 2013) for a detailed discussion).

Remark 1. When convenient, the identified (minimal) model G_0 is written in terms of its associated state-space representation, *i.e.* $G_0(s) = C_0(s\mathbb{I} - A_0)^{-1}B_0$ where

$$\dot{x} = A_0 x + B_0(d-u), \quad y = C_0 x, \tag{9}$$

with $x(t) \in \mathbb{R}^n$ the state-vector of the nominal WEC system, and where the triple of matrices (A_0, B_0, C_0) is conformable for (9).

Following the identification of the nominal model as per (8), and given the nature of the space $\mathcal{D}$, the uncertainty weight W_Δ can be defined by simply leveraging the following condition:

$$|W_\Delta(\jmath\omega)| \geq r_\Delta(\omega) = \max_{i\in\mathbb{N}_Q} \left|\bar{G}_i(\jmath\omega) - G_0(\jmath\omega)\right|, \tag{10}$$

where the map r_Δ denotes the smallest radius including all possible plants in $\mathcal{G}$. A corresponding parametric description $W_\Delta(s)$, fulfilling (10), can be performed by exploiting standard filter realisation techniques (see (Ljung, 1999)).

The results of this experimental uncertainty characterisation procedure, for the Wavestar prototype, are summarised within the Bode diagram presented in Figure 2. In particular, as per (Celesti et al., 2024), the results discussed in the following are obtained by imposing a set of input signals $\mathscr{F}$, composed of banded white-noise waves generated within the basin using the available wavemaker, with significant energy content covering the full operating range of the prototype. Figure 2 (top) illustrates the magnitude associated with each ETFE G_i, and that characterising the identified nominal WEC model G_0 (order/dimension 4), while Figure 2 (bottom) offers an appraisal of the map r_Δ, and the identified uncertainty weight W_Δ (order/dimension 2), fulfilling (10).

NOMINAL AND ROBUST CONTROL DESIGN

Within this section, and following the discussion pursued in Section "Introduction" , we provide a definition of the control problem for WEC systems, in both nominal and uncertain conditions. In particular, the overall aim of WEC control technology is that of maximising the energy absorbed from the incoming wave field, which, in a nominal scenario, can be essentially written in terms of a (correspondingly nominal) OCP, termed $(P)_0$, as

$$\begin{aligned}(P)_0 : u_0^{\text{opt}} &= \arg\max_u \frac{1}{T}\langle u, y\rangle_\Omega,\\ &\text{subject to:}\\ &Y = G_0(D-U),\\ &(u,p) \in \mathcal{U}\times\mathcal{P}, \quad \forall t \in \Omega\end{aligned} \tag{11}$$

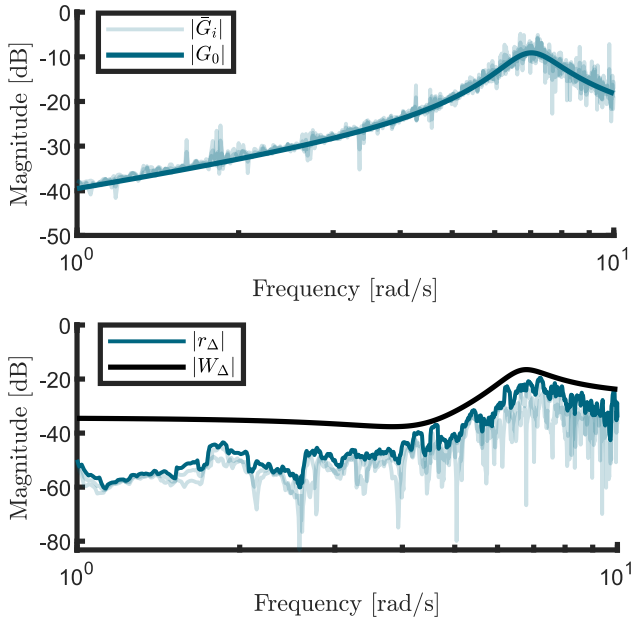

Fig. 2 Frequency-domain characterisation of the family of systems $\mathcal{G}$, describing the experimental WEC prototype considered within this study.

where $\Omega = [0\ T] \subset \mathbb{R}^+$ is the time interval in which energy is effectively maximised, u_0^{opt} denotes the associated nominal optimal control input, and, for the considered Wavestar prototype, $p = \int y$ denotes the angular position of the WEC system about the reference point in Figure 1. The admissible sets $\mathcal{U}$ and $\mathcal{P}$, which enforce fulfilment of technological constraints in available control effort and maximum operational space, respectively, are defined in terms of standard box (∞-norm) constraints, *i.e.*

$$\mathcal{U} : \{u \in \mathbb{R} \mid |u| \leq U_{\max}\}, \quad \mathcal{P} : \{p \in \mathbb{R} \mid |p| \leq P_{\max}\}, \tag{12}$$

where $(U_{\max}, P_{\max}) \in \mathbb{R}^+ \times \mathbb{R}^+$ denote maximum admissible values for control torque and angular displacement, accordingly.

Remark 2. Note that the equality constraint describing the dynamics of the WEC system within the OCP defined in (11) does not contain any information regarding deviations from the nominal operator G_0, *i.e.* it provides a control solution in idealised (nominal) conditions. To incorporate such information, the OCP has to be instead defined in terms of the family of systems (5), hence effectively including dynamical uncertainty when solving for the corresponding optimal control input.

In the light of Remark 2, and following the underlying principles presented in (Ben-Tal et al., 2009), we pursue a worst-case paradigm, in which the nominal OCP $(P)_0$ is re-casted in terms of an associated robust optimisation formulation, that is, in line with Wald's decision principle:

$$\begin{aligned}(P)_{\text{R}} : u_{\text{R}}^{\text{opt}} = \arg\max_{u}\ \arg\min_{G\in\mathcal{G}}\ & \frac{1}{T}\langle u, y\rangle_\Omega, \\ \text{subject to:}\ & \\ Y = G(D-U),\ & \\ (u,p) \in \mathcal{U}\times\mathcal{P}, \quad & \forall t \in \Omega \wedge G \in \mathcal{G}.\end{aligned} \tag{13}$$

The OCP presented in $(P)_{\text{R}}$ is written in terms of a maximin procedure which, for a given wave excitation d, computes a solution $u_{\text{R}}^{\text{opt}}$ maximising the worst-case performance in terms of energy absorption, for every possible dynamical WEC description $G \in \mathcal{G}$, while consistently respecting the set of technological constraints for any potential plant in (5).

Clearly, both the nominal OCP formulation $(P)_0$ in (11), and its corresponding robust counterpart $(P)_{\text{R}}$ in (13), are defined over infinite-dimensional function spaces, necessitating a suitable approximation technique to compute its solution. To produce a computationally tractable problem, we consider, within this study, the direct transcription approach presented in (Faedo and Ringwood, 2023), based on the mathematical concept of a *moment* (see also the discussion provided in Section "Introduction"). Moments are, in essence, a system-theoretic characterisation of the steady-state response of a dynamical map, excited by a user-defined class of input signals. In particular, within such a moment-based framework, we consider that both control u and disturbance (wave excitation torque) d can be expressed in terms of a finite number of harmonics of a given fundamental frequency $\omega_0 = 2\pi/T$, written using an associated exogenous system, commonly termed *signal generator*, *i.e.*

$$\dot{\zeta} = S\zeta, \quad u = L_u\zeta, \quad d = L_d\zeta, \tag{14}$$

where $\lambda(S) = \{\pm\jmath k\omega_0\}_{k\in\mathbb{N}_{\nu/2}} \subset \mathbb{C}^0$, with $\nu \in 2\mathbb{Z}$, $\zeta(t) \in \mathbb{R}^\nu$, while $\left(S, L_u^\intercal, L_d^\intercal\right) \in \mathbb{R}^{\nu\times\nu} \times \mathbb{R}^\nu \times \mathbb{R}^\nu$. The system in (14) is assumed to be driven by a suitably defined initial condition $\zeta(0) = \zeta_0$, where the pair (S, ζ_0) is reachable.

With the definition of the signal generator in (14), and the corresponding device state-space description in (9), the steady-state response y_0^{ss} of the nominal WEC system G_0 can be computed in terms of the unique solution of an invariant manifold (Sylvester) equation (see (Faedo and Ringwood, 2023)), which, after suitable algebraic manipulation, can be written as

$$\begin{aligned} y_0^{\text{ss}} &= \underline{\Upsilon}_0\zeta, \\ \underline{\Upsilon}_0 &= \Phi_0(L_d - L_u), \\ \Phi_0^\intercal &= (\mathbb{I}_\nu \otimes C_0)\left(S\otimes\mathbb{I}_n + \mathbb{I}_\nu\otimes A_0\right)^{-1}(\mathbb{I}_\nu\otimes -B_0). \end{aligned} \tag{15}$$

Furthermore, if the matrix S, characterising the internal dynamics of the exogenous generator in (14), is written (without any loss of generality) in a Jordan canonical form over $\mathbb{R}$, *i.e.*

$$S = \bigoplus_{k\in\mathbb{N}_{\nu/2}} \begin{bmatrix} 0 & k\omega_0 \\ -k\omega_0 & 0 \end{bmatrix}, \tag{16}$$

it is relatively straightforward to prove (see (Faedo, 2020)) that the matrix Φ_0 in (15) can be alternatively written in terms of the nominal frequency-response function $G_0(\jmath\omega)$, *i.e.*

$$\Phi_0 = \bigoplus_{k\in\mathbb{N}_{\nu/2}} \mathscr{B}(\phi_0^k), \quad \text{with } \phi_0^k = G_0(\jmath k\omega_0). \tag{17}$$

Remark 3. Equation (17) facilitates, in essence, a direct relation between the frequency-domain experimental characterisation of the WEC prototype, discussed in Section "Device and uncertainty description" , and the moment-based approach pursued for direct transcription of the associated OCP, as presented within the remainder of this section.

Up until this point, equations (15)-(16)-(17) describe a moment-based representation of the steady-state response of the WEC system in its nominal conditions, *i.e.* without considering the presence of modelling uncertainty. To incorporate this information within the same framework, let $H_\Delta = W_\Delta\Delta$, for any admissible Δ in $\mathcal{D}$. Following an analogous procedure to that pursued

in (Faedo, 2020), and leveraging the equality in (17), the steady-state response y^{ss} of the (actual) WEC system $G \in \mathcal{G}$, for any fixed Δ, can be written in terms of the solution of (14) as

$$\begin{aligned} y^{\mathrm{ss}} &= (\underline{\mathrm{Y}}_0 + \underline{\mathrm{Y}}_\Delta)\,\zeta, \\ \underline{\mathrm{Y}}_\Delta &= \Phi_\Delta(L_d - L_u), \\ \Phi_\Delta &= \bigoplus_{k \in \mathbb{N}_{\nu/2}} \mathscr{B}(\phi_\Delta^k), \quad \text{with } \phi_\Delta^k = H_\Delta(\jmath k \omega_0). \end{aligned} \tag{18}$$

Remark 4. Note that $\underline{\mathrm{Y}}_\Delta$ effectively encodes the information regarding the uncertainty affecting the nominal model G_0 at the frequency points induced by $\lambda(S)$, *i.e.* $\{\jmath k\omega_0\}_{k\in\mathbb{N}_{\nu/2}}$, particularly by means of the matrix Φ_Δ in (18).

Given the identified uncertainty weight W_Δ, characterising the family (5), and with the main objective of translating the experimentally computed bound condition (10) to the corresponding moment-based transcription (18), we begin by noting that

$$|\phi_\Delta^k| \leq |W_\Delta(\jmath k\omega_0)|, \quad \forall k \in \mathbb{N}_{\nu/2}, \tag{19}$$

as a direct consequence of (10). Furthermore, considering the inequality in (19), let $\{\delta_{++}^k, \delta_{+-}^k, \delta_{-+}^k, \delta_{--}^k\} \subset \mathbb{R}^2$ be defined as

$$\begin{aligned} \delta_{++}^k &= \mathscr{R}(\phi_0^k) + |W_\Delta(\jmath k\omega_0)| \begin{bmatrix} 1 & 1 \end{bmatrix}^{\mathsf{T}}, \\ \delta_{+-}^k &= \mathscr{R}(\phi_0^k) + |W_\Delta(\jmath k\omega_0)| \begin{bmatrix} 1 & -1 \end{bmatrix}^{\mathsf{T}}, \\ \delta_{-+}^k &= \mathscr{R}(\phi_0^k) + |W_\Delta(\jmath k\omega_0)| \begin{bmatrix} -1 & 1 \end{bmatrix}^{\mathsf{T}}, \\ \delta_{--}^k &= \mathscr{R}(\phi_0^k) + |W_\Delta(\jmath k\omega_0)| \begin{bmatrix} -1 & -1 \end{bmatrix}^{\mathsf{T}}, \end{aligned} \tag{20}$$

for every $k \in \mathbb{N}_{\nu/2}$.

Remark 5. Note that this set of vectors can be effectively used to describe the corresponding modelling uncertainty for each single frequency point induced by $\lambda(S)$ in terms of a box-type bound, as schematically illustrated in Figure 3 (left).

The definitions provided in (20) characterise deviations from the nominal model associated with a single point in frequency, *i.e.* according to a single element in $\lambda(S)$. In order to effectively reflect and cover any potential dynamical deviations from the corresponding nominal WEC model, for the full set $\{\jmath k\omega_0\}$, we define the following set $\mathscr{V} \subset \mathbb{R}^\nu$ of bounding vertexes:

$$\begin{aligned} \mathscr{V} &= \{V_{++}, V_{+-}, V_{-+}, V_{--}\}, \\ V_{++} &= \begin{bmatrix} \delta_{++}^{1^{\mathsf{T}}} & \dots & \delta_{++}^{\nu/2^{\mathsf{T}}} \end{bmatrix}^{\mathsf{T}}, \quad V_{+-} = \begin{bmatrix} \delta_{+-}^{1^{\mathsf{T}}} & \dots & \delta_{+-}^{\nu/2^{\mathsf{T}}} \end{bmatrix}^{\mathsf{T}}, \\ V_{-+} &= \begin{bmatrix} \delta_{-+}^{1^{\mathsf{T}}} & \dots & \delta_{-+}^{\nu/2^{\mathsf{T}}} \end{bmatrix}^{\mathsf{T}}, \quad V_{--} = \begin{bmatrix} \delta_{--}^{1^{\mathsf{T}}} & \dots & \delta_{--}^{\nu/2^{\mathsf{T}}} \end{bmatrix}^{\mathsf{T}}, \end{aligned} \tag{21}$$

which essentially contains all the limit points characterising the box-type bounds for each frequency (eigenvalue) in the signal generator (14), as illustrated within Figure 3 (right). Note that the set $\mathscr{V}$ induces a corresponding (uniquely defined) convex $\mathscr{V}$-polytope in $\mathbb{R}^\nu$, *i.e.* $\mathscr{O} = \mathrm{conv}(\mathscr{V})$, which fully covers any potential deviations from the nominal response ϕ_0^k, for any $k \in \mathbb{N}_{\nu/2}$, according to the bounding condition (19).

Following the definition of the set $\mathscr{V}$ in (21), and the induced polytope $\mathscr{O}$, let now $\phi^k = \phi_0^k + \phi_\Delta^k$, which essentially corresponds with the frequency response of the actual WEC plant for any given uncertainty Δ, according to $\lambda(S)$ in (14). Furthermore, let us 'collect' these values in terms of an associated response vector

$$V_\phi = \begin{bmatrix} \mathscr{R}(\phi^1)^{\mathsf{T}} & \dots & \mathscr{R}(\phi^{\nu/2})^{\mathsf{T}} \end{bmatrix}^{\mathsf{T}} \in \mathbb{R}^\nu. \tag{22}$$

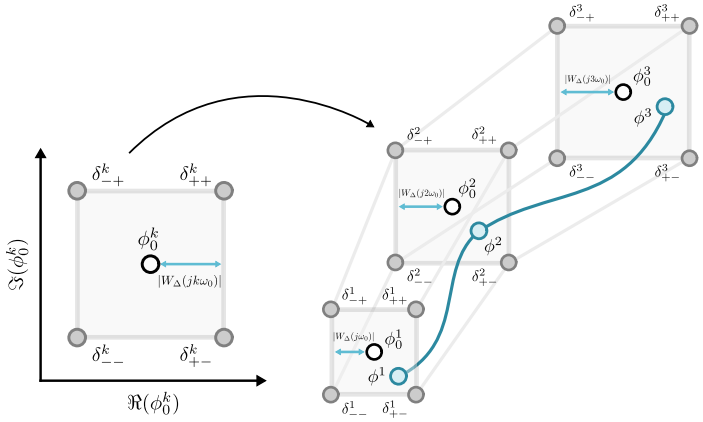

Fig. 3 Geometric description of the considered uncertainty sets, for a single frequency (left), and a subset of points (right), induced by $\lambda(S)$. Grey circles denote (limit) vertexes, while black and blue circles denote nominal and actual response, according to the family of WEC systems (5).

Leveraging the definition in (22), it is possible to see that the moment-based representation of the actual (uncertain) WEC plant in (18) can be compactly written in terms of V_ϕ as

$$\begin{aligned} y^{\mathrm{ss}} &= \underline{\mathrm{Y}}\zeta, \\ \underline{\mathrm{Y}} &= (L_d - L_u) \bigoplus_{k \in \mathbb{N}_{\nu/2}} \mathscr{B}(\phi^k). \end{aligned} \tag{23}$$

Remark 6. From (22)-(23), it is straightforward to see that $V_\phi \in \mathscr{O}$ for any admissible uncertainty element, *i.e.* $\forall \Delta \in \mathcal{D}$. That is, any possible variation from the nominal moment in (15) can be covered (and represented) in terms of the convex polytope $\mathscr{O}$.

Finally, considering the parametric representation of the steady-state response via moments in (14)-(23), the robust OCP formulation $(P)_{\mathrm{R}}$ can be fully transcribed into an approximating finite-dimensional nonlinear program in $\mathbb{R}^\nu$ as[1]

$$\begin{aligned} \widetilde{(P)}_{\mathrm{R}} : L_{u_{\mathrm{R}}} = \arg \max_{L_u^{\mathsf{T}} \in \mathbb{R}^\nu} \ \arg \min_{V_\phi \in \mathscr{V} \subset \mathscr{O}} \ & \frac{1}{T} \langle L_u\zeta, \underline{\mathrm{Y}}\zeta \rangle_\Omega, \\ \text{subject to:} \\ & \underline{\mathrm{Y}} = \mathscr{B}(V_\phi)(L_d - L_u), \\ & (L_u\zeta, \underline{\mathrm{Y}}S^{-1}\zeta) \in \mathcal{U} \times \mathcal{P}, \quad \forall t \in \Omega_{\mathrm{c}} \wedge V_\phi \in \mathscr{V}, \end{aligned} \tag{24}$$

where the associated robust control solution is $u_{\mathrm{R}} = L_{u_{\mathrm{R}}}\zeta$. The set of technological constraints in (13) are collocated by means of the set of N_{c} uniformly distributed instants $\Omega_{\mathrm{c}} = \{t_i\}_{i\in\mathbb{N}_{N_{\mathrm{c}}}} \subset \Omega$.

Remark 7. Tractability of (24) can be guaranteed by exploiting the theoretical results in (Faedo, 2020). In particular, it can be shown that (24) is quadratically concave in the controller parameterisation L_u (for any physically meaningful WEC family $\mathcal{G}$) and linear in the response vector V_ϕ, which implies that is sufficient to solve $\widetilde{(P)}_{\mathrm{R}}$ at the four vertexes defining the polytope $\mathscr{O}$, *i.e.* $\mathscr{V}$. This guarantees both a robust solution in the sense of optimal energy absorption in the worst-case scenario, and consistent constraint satisfaction, for any V_ϕ, due to the convexity of $\mathscr{O}$.

[1] Variable integration, in terms of the exogenous system (14), can be simply performed by matrix inversion, *i.e.* if $y^{\mathrm{ss}} = \underline{\mathrm{Y}}\zeta$, then $p^{\mathrm{ss}} = \underline{\mathrm{Y}}S^{-1}\zeta$ (see (Faedo, 2020)).

Remark 8. If $\Delta = 0$ in (4), *i.e.* we exclude uncertainty and compute the corresponding optimal controller solely based on a nominal WEC model, then the formulation in (24) can be effectively used to derive a nominal moment-based control solution in a straightforward fashion, *i.e.* in terms of the nonlinear program

$$\begin{aligned}\widetilde{(P)}_0 : L_{u_0} = \arg \max_{L_u^{\mathrm{T}} \in \mathbb{R}^{\nu}} \ & \frac{1}{T}\langle L_u\zeta, \underline{Y}_0\zeta\rangle_{\Omega}, \\ \text{subject to:} \quad & \\ \underline{Y}_0 = \ & \Phi_0(L_d - L_u), \\ (L_u\zeta, \underline{Y}S^{-1}\zeta) \in \ & \mathcal{U} \times \mathcal{P}, \quad \forall t \in \Omega_{\mathrm{c}},\end{aligned} \tag{25}$$

where the corresponding nominal control torque is $u_0 = L_{u_0}\zeta$.

NUMERICAL RESULTS

This section presents a numerical appraisal of the overall results obtained, considering the family of uncertain WEC models for the tested Wavestar prototype system, computed as described in Section "Device and uncertainty description" . In particular, aiming to test both nominal and robust control synthesis procedures, and hence provide an assessment of the effect that uncertainty can effectively have in the overall device production under controlled conditions, 300 plants in $\mathcal{G}$ are generated according to the experimental characterisation presented in Section "Device and uncertainty description" , by a corresponding random sampling from $\mathcal{D}$, for exhaustive simulation. Each of these randomly generated systems in $\mathcal{G}$ are represented in terms of a Nyquist plot, within Figure 4, using blue lines with transparency.

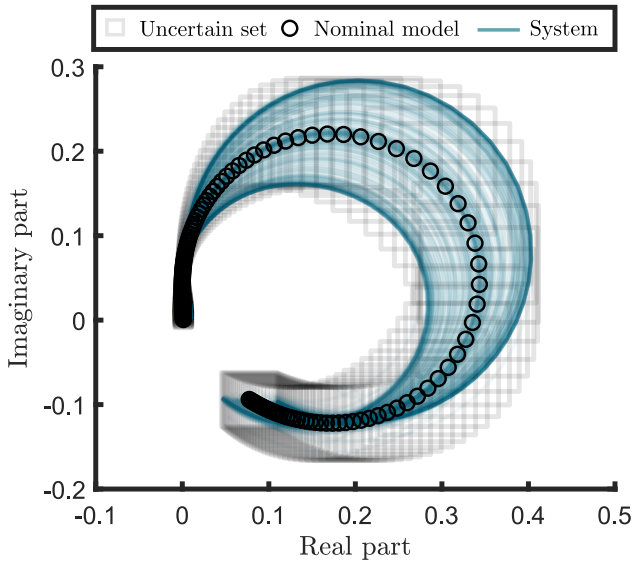

Fig. 4 Nyquist plot for the randomly sampled elements from the family $\mathcal{G}$ (transparent-blue lines), nominal response (circles) at the frequencies induced by $\lambda(S)$, and corresponding uncertainty for each single element (squares).

A single sea-state condition is considered for performance assessment, generated within the wave basin using a JONSWAP description with $H_s = 0.0624$ [m], $T_p = 0.988$ [s], and $\gamma = 1$, being this a wide-banded operating condition, with a typical period close to the device resonance. The length of the generated wave is set to $T = 100$ [s] (which corresponds to ≈ 100 typical peak periods). While the measured wave torque is effectively used for simulation purposes, within moment-based theory, an approximation of d is pursued in terms of the exogenous system in (14), which defines the optimisation space for both robust and nominal direct transcription procedures in (24) and (25), respectively.

To get an accurate description of both wave and uncertainty sets within such a moment-based direct transcription procedure, we set $\nu = 320$ in (16), which corresponds to 160 harmonics of the fundamental frequency $\omega_0 = 2\pi/100$ [rad/s]. Both the nominal system response and corresponding uncertainty set (defined in terms of the set of vertexes (20), for each frequency induced by $\lambda(S)$, are also represented within Figure 4. The corresponding uncertainty $\mathscr{V}$-polytope, defined in terms of (21), can be derived directly from the vertexes defined in (20), as per Figure 4.

Figure 5 provides an appraisal of both the (measured) wave excitation force d, generated within the basin, and the corresponding nominal u_0 (blue) and robust u_{R} (black) control solutions, according to the uncertainty characterisation (and associated family of WEC models) presented in Figure 4. For this particular analysis, both control solutions have been computed in an unconstrained scenario, *i.e.* $\mathcal{U} = \mathcal{P} \equiv \mathbb{R}$ in (24) and (25), to purely assess overall energy-maximising performance. Note that the resulting control torques are indeed significantly different, including a relatively large change in maximum applied force (and corresponding variance), being the robust case more conservative in terms of applied control effort than its nominal counterpart.

The performance obtained when applying these two control solutions to each of the randomly sampled 300 members of the experimentally characterised family $\mathcal{G}$ (see Figure 4) can be appreciated in the histogram of Figure 6. The results presented within this figure elucidate quite a concerning conclusion: While the nominal control solution is sometimes able to achieve higher values of mean power when compared to its robust counterpart, it can also produce negative energy absorption for a relatively large number of cases within $\mathcal{G}$, effectively draining power from the grid, as opposed to increasing generation. In other words, the variability in terms of performance is significantly large, hindering a consistent power generation across $\mathcal{G}$. In contrast, the robust solution, while more conservative, is able to narrow the distribution of generated mean power by leveraging knowledge of the uncertainty affecting the process, being largely more consistent than its nominal formulation, always delivering positive energy generation, for any $G \in \mathcal{G}$.

Finally, and to showcase the fundamental issue of constraint satisfaction in uncertain scenarios, both nominal and robust control solutions are re-computed, for the same wave excitation d, but now considering a corresponding constraint in device angular displacement, with $P_{\max} = 20$ [deg] in (12). The collocation set Ω_{c}, used to enforce constraint satisfaction in (24) and (25), is composed of uniformly distributed time instants with a corresponding sampling of 0.05 [s], resulting in a cardinality of $N_{\mathrm{c}} = 4000$. A preliminary, yet significantly strong, result, is presented in Figure 7, which illustrates a time-snippet of device motion under nominal (solid blue) and robust (dotted black) control actions, for the totality of the randomly sampled WEC systems in $\mathcal{G}$ considered. As can be appreciated directly from the figure, the robust control solution is able to systematically respect the defined constraint set by effectively exploiting the knowledge of the uncertainty polytope $\mathscr{O}$, while its nominal counterpart, only informed

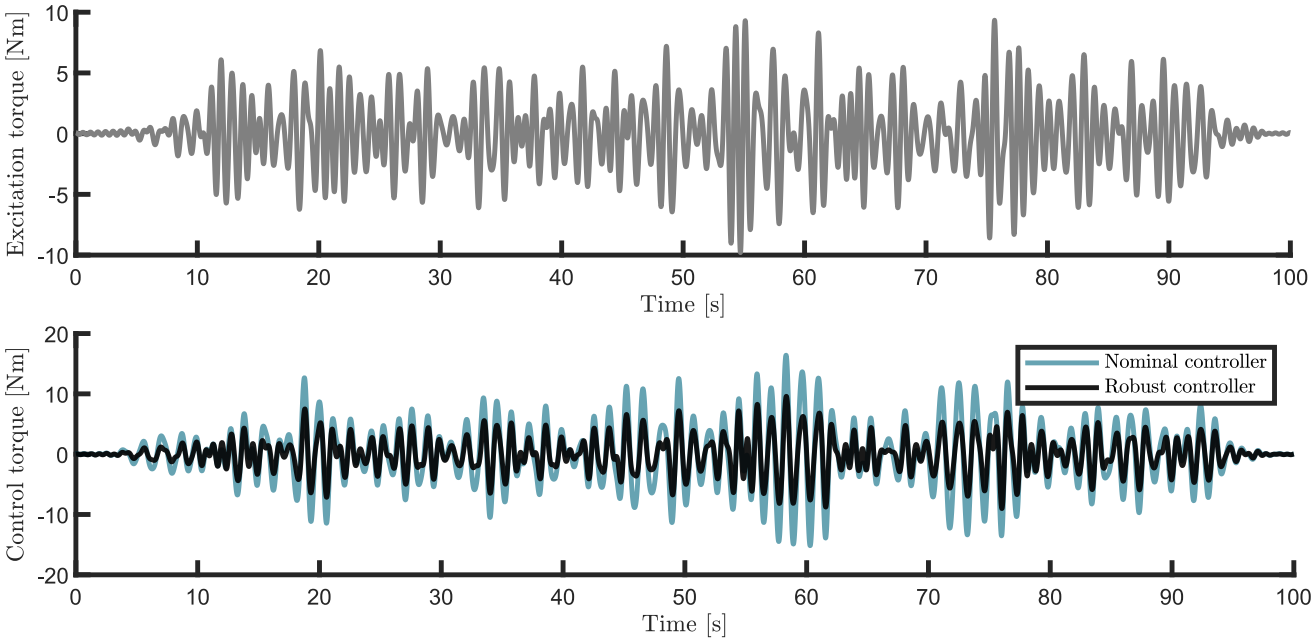

Fig. 5 Measured wave excitation torque generated within the wave tank (top), and corresponding nominal u_0 (solid blue) and robust u_R (solid black) control inputs (bottom).

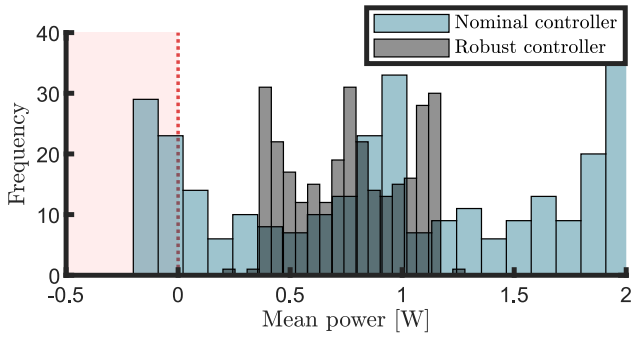

Fig. 6 Histogram of the performance obtained with nominal (blue) and robust (black) control solutions, considering the set of 300 randomly sampled systems in $\mathcal{G}$.

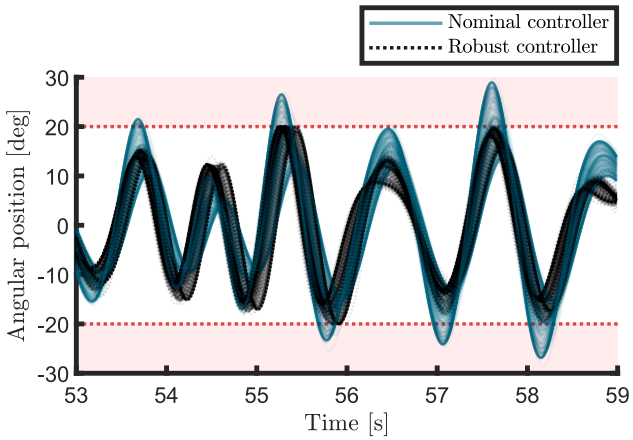

Fig. 7 Time-snippet of device motion under nominal (solid blue) and robust (dotted black) control actions, for the totality of the randomly sampled WEC systems in $\mathcal{G}$ considered.

by the nominal WEC model, does not guarantee the imposed technological limits. This is illustrated in a more complete fashion within Figure 8, which presents, in sampling counts, the absolute value of angular displacement for each simulated WEC system, in nominal (solid blue) and robust (dotted black) control scenarios. The difference between these two solutions is evident, being the robust counterpart able to fulfil the designed limits consistently, in spite of the presence of uncertainty. This is not the case for the nominal controller, which spends a (quite) elevated number of sampling instants outside the constraint set itself, potentially generating a fatigue excess in device components, reducing its overall lifetime, and increasing maintenance requirements.

CONCLUSIONS

Consistent and accurate modelling of wave energy systems is a difficult task, mainly due to the strong hydrodynamic component within the description of the energy absorption process itself. Linear models are widely used for energy-maximising control purposes, ostensibly due to their underlying computational (and representational) simplicity. Nonetheless, a significant degree of uncertainty is introduced when adopting this practice, due to relevant unmodelled effects. This issue translates directly to model-based design, though this is virtually always ignored within the current WEC control and device assessment literature.

A more complete panorama can be obtained when quantifying uncertainty properly, in terms of tailored experiments, and a corresponding (suitably defined) family of WEC systems. Within this paper, and to showcase the overall effect of modelling uncertainty in the overall control design and performance assessment procedure, a family of models is computed based on exper-

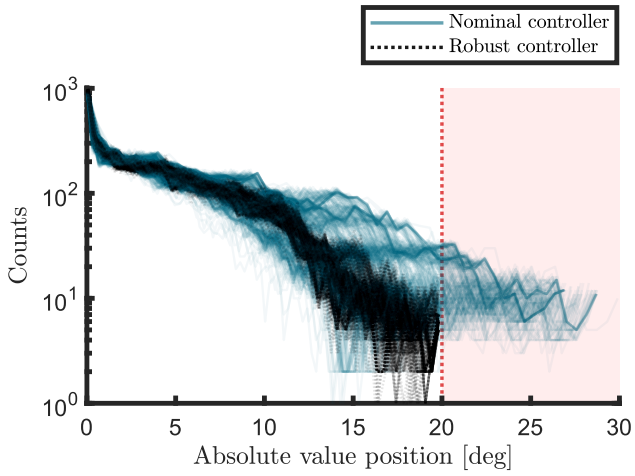

Fig. 8 Absolute value of angular displacement (in sampling counts), for each of the 300 randomly sampled simulated WEC systems, in nominal (solid blue) and robust (dotted black) control scenarios.

imental data, for a 1:20 scale Wavestar prototype. Furthermore, leveraging state-of-the-art direct transcription techniques, particularly moment-based control, we design and synthesise optimal controllers in nominal and uncertain (robust) scenarios. We explicitly demonstrate that neglecting uncertainty can lead to two fundamental issues: Inconsistent performance, even draining, as opposed to generating, energy from the grid, and failure to fulfil technological limitations. These two significant problems can certainly compromise the role of control technology in lowering the associated LCoE, due to (a) suboptimal energy absorption performance and (b) increased device fatigue due to inconsistent constraint satisfaction, affecting scheduled maintenance and reducing the overall lifetime of the device.

Fortunately, it's not all bad news: We further show that, if a suitable mathematical framework is exploited accordingly, informing the control synthesis procedure on the existence of uncertainty, and a corresponding set of suitably defined bounds, guarantees a consistent energy absorption performance with a remarkable reduction in variability and systematic constraint satisfaction, hence recovering the role of this technology in helping towards WEC commercialisation.

REFERENCES

Bacelli, G., Genest, R., and Ringwood, J. V. (2015). "Nonlinear control of flap-type wave energy converter with a non-ideal power take-off system." *Annual Reviews in Control*, 40, 116–126.

Ben-Tal, A., El Ghaoui, L., and Nemirovski, A. (2009). *Robust optimization*, volume 28. Princeton university press.

Celesti, M. L., Ferri, F., and Faedo, N. (2024). "Experimental modelling uncertainty quantification for a prototype wave energy converter." In *European Control Conference (ECC), Under review, Stockholm*, 1–6.

Clément, A., McCullen, P., Falcão, A., Fiorentino, A., Gardner, F., Hammarlund, K., Lemonis, G., Lewis, T., Nielsen, K., Petroncini, S., et al. (2002). "Wave energy in Europe: current status and perspectives." *Renewable and Sustainable Energy Reviews*, 6(5), 405–431.

Faedo, N. (2020). *Optimal control and model reduction for wave energy systems: A moment-based approach*. PhD thesis, Department of Electronic Engineering, Maynooth University.

Faedo, N., Giorgi, G., Ringwood, J. V., and Mattiazzo, G. (2022a). "Nonlinear moment-based optimal control of wave energy converters with non-ideal power take-off systems." In *Proc. ASME Int. Conf. on Offshore Mechanics and Arctic Engineering, Hamburg*, volume 85932, V008T09A082.

Faedo, N., Mattiazzo, G., and Ringwood, J. V. (2022b). "Robust energy-maximising control of wave energy systems under input uncertainty." In *2022 European Control Conf. (ECC)*, 614–619. IEEE.

Faedo, N., Pasta, E., Carapellese, F., Orlando, V., Pizzirusso, D., Basile, D., and Sirigu, S. A. (2022c). "Energy-maximising experimental control synthesis via impedance-matching for a multi degree-of-freedom wave energy converter." *IFAC-PapersOnLine*, 55(31), 345–350.

Faedo, N., Peña-Sanchez, Y., Pasta, E., Papini, G., Mosquera, F. D., and Ferri, F. (2023). "SWELL: An open-access experimental dataset for arrays of wave energy conversion systems." *Renewable Energy*, 212, 699–716.

Faedo, N. and Ringwood, J. V. (2023). "A Control Framework for Ocean Wave Energy Conversion Systems: The Potential of Moments." *Annual Review of Control, Robotics, and Autonomous Systems*, 7.

Farajvand, M., Grazioso, V., García-Violini, D., and Ringwood, J. V. (2023). "Uncertainty estimation in wave energy systems with applications in robust energy maximising control." *Renewable Energy*, 203, 194–204.

Garcia-Violini, D. and Ringwood, J. V. (2021). "Energy maximising robust control for spectral and pseudospectral methods with application to wave energy systems." *International Journal of Control*, 94(4), 1102–1113.

Hansen, R. H. and Kramer, M. M. (2011). "Modelling and control of the Wavestar prototype." In *9th European Wave and Tidal Energy Conference (EWTEC), Southampton*, 1–10.

Korde, U. A. and Ringwood, J. (2016). *Hydrodynamic control of wave energy devices*. Cambridge University Press.

Ljung, L. (1999). *System identification: Theory for the User (2nd ed.)*. Prentice-Hall.

Pasta, E., Faedo, N., Mattiazzo, G., and Ringwood, J. V. (2023). "Towards data-driven and data-based control of wave energy systems: Classification, overview, and critical assessment." *Renewable and Sustainable Energy Reviews*, 188, 113877.

Ringwood, J. V., Tom, N., Ferri, F., Yu, Y.-H., Coe, R. G., Ruehl, K., Bacelli, G., Shi, S., Patton, R. J., Tona, P., et al. (2023a). "The wave energy converter control competition (WECCCOMP): Wave energy control algorithms compared in both simulation and tank testing." *Applied Ocean Research*, 138, 103653.

Ringwood, J. V., Zhan, S., and Faedo, N. (2023b). "Empowering wave energy with control technology: Possibilities and pitfalls." *Annual Reviews in Control*.

Scruggs, J., Lattanzio, S., Taflanidis, A., and Cassidy, I. (2013). "Optimal causal control of a wave energy converter in a random sea." *App. Ocean Res.*, 42, 1–15.

Windt, C., Faedo, N., Penalba, M., Dias, F., and Ringwood, J. V. (2021). "Reactive control of wave energy devices–the modelling paradox." *Applied Ocean Research*, 109, 102574.

Zhang, Y. and Li, G. (2022). "Robust Tube-Based Model Predictive Control for Wave Energy Converters." *IEEE Trans. on Sust. Energy*, 14(1), 65–74.